Surface structure of CoCrMo and Ti6Al4V parts obtained by selective laser sintering

V. DESPA[a*], A. CATANGIU[a], D.N. UNGUREANU[a], I.A. IVAN[a]
[a]*Valahia University of Targoviste, 2 Regele Carol I Street, Targoviste, Romania*

Based on a three-dimensional computer-aided design model, selective laser sintering technology has been used to manufacture parts from CoCrMo and Ti6Al4V. Knowing the biocompatible characteristics of both materials, the parts surfaces have been analyzed by SEM and surface profilometry, in order to further investigate their potential for bioactive coating substrates. Due to the specific conditions of laser sintering (surface anisotropy along the z axis) both lateral and top surfaces were analyzed. Top surface roughness ($R_{a\ top}$=0.244 µm; R_a – the average absolute deviation from the mean line over sampling length) of CoCrMo sample is significant lower than lateral surface roughness one ($R_{a\ lateral}$=2.553 µm). In case of Ti6Al4V sample, lateral and top surfaces structures are similar, and the roughness of these surfaces are significantly close ($R_{a\ lateral}$=0.751 µm; $R_{a\ top}$ =1.073 µm).

(Received March 25, 2013; accepted July 11, 2013)

Keywords: Rapid prototyping, Selective laser sintering, CoCrMo alloy, Ti6Al4V alloy, Surface topography

1. Introduction

Most materials used as implants are subjected to dynamic loads and this condition requires a good combination of strength and ductility. The efficacy of artificial implants is determined mainly by their surface characteristics such as surface morphology, microstructure and composition [1-3].

Titanium alloy or CoCr alloy are two classes of biocompatible materials with high strength which can be used as substrate for biocompatible thin films such as hydroxyapatite films [4-6]. The mechanical strength of this kind of composite structure is provided by substrate and biocompatibility by hydroxyapatite [7].

There can be used various methods of part manufacturing which are used as substrate, but the minimum time between concept and finished product is achieved by the rapid prototyping technologies such as selective laser sintering.

Selective laser sintering is a manufacturing process based on layer-by-layer deposition in which the part is built up based on a 3D CAD model. By using appropriate software, the model is divided in horizontal cross-sections which are sequentially created on a substrate. The alloys in the form of powder are melted directly with a laser beam and create layer by layer a solid, three-dimensional object.

The surface quality of the parts is lower than that of the machined ones due to the fusion process [8] and is limited by the stair-step effect and the particle size of the powder [9, 10].

The influence of surface roughness on the rate of biomechanical fixation of hard tissue implants has been identified as a key factor.

This observation also leads to the conclusion that hard tissue implants based on alloys, mainly titanium, were not only entirely bioinert or biocompatible, but proper surface conditioning could also influence tissue response and this in turn could be exploited to achieve a higher level of biocompatibility [11].

Better results are obtained in case of substrates with high specific surface. For this purpose, various methods of increasing the specific surface, such us laser surface modification for the deposition of hydroxyapatite by pulsed laser deposition [12] have been used, specific surface value being directly linked with the roughness one. Laser induced surface topography changes can be further explored to improve the functionality of implants.

2. Materials and methods

In the present work, a selective laser sintering process developed by the company EOS has been used for obtaining CoCrMo and Ti6Al4V sample parts.

Fig. 1. Direct Metal Laser Sintering machine EOSINT M270 - National Institute for Research and Development in Mechatronics and Measurement Technique (INCDMTM) Bucharest.

The experiments shown in this paper were carried out using EOS CobaltChrome MP1 (a multi-purpose cobalt-chrome-molybdenum based superalloy) and EOS Titanium Ti64 powders which have been optimized especially for processing on EOSINT M270 systems (Fig. 1). Both materials are ideal for many part-building applications such as functional metal prototypes or individualized products, such as those in Fig. 2 which are intended for a bio-medical gripper.

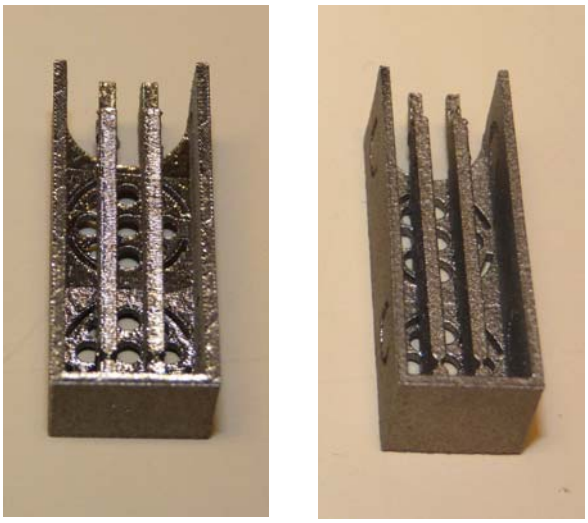

a. CoCrMo *b. Ti6Al4V*

Fig. 2. Sample parts configuration

In order to investigate the surface quality of these materials profilometry and scanning electron microscopy analysis were performed.

The average surface roughness (R_a) was measured by profilometry at random locations over lateral and top surfaces using a TENCOR Alpha-Step IQ system.

The target parameter of the surface quality analysis is the surface roughness average R_a, which is defined as arithmetic average of the roughness profile over the total measured length and R_q which is defined as root mean squared of the same values.

Microstructural analyses were performed using a JEOL SEM in the Femto-ST Institute from Besançon, France.

3. Results and discution

3.1. Structural analysis of CoCrMo part

As may be seen in Fig.3, the laser beam scan entire work surface after a path controlled by software, during the sample construction. Workpiece surface appearance also suggests a beam sweep along its contour (Fig.3, Fig. 4).

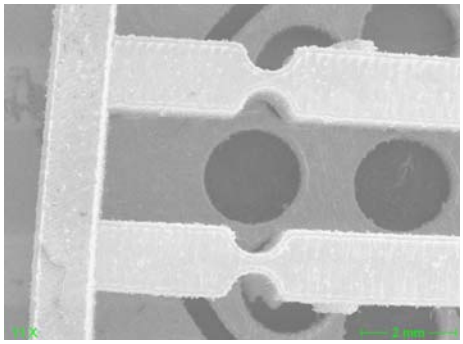

Fig.3. CoCrMo part (SEM - top surface)

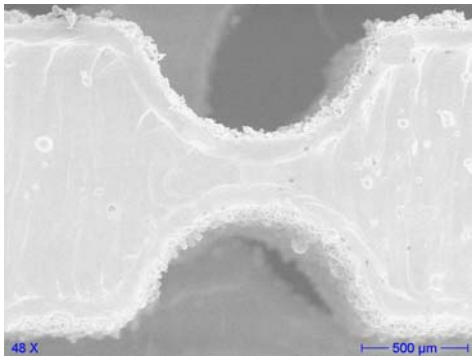

Fig.4. CoCrMo part (SEM detail - top surface)

The lateral surface of part looks rough, surface roughness is more pronounced compared to the top side which will be show in Fig. 5, Fig.10 and Table 1. Top surface roughness ($R_{a\ top}$=0.244 µm) is significant lower than lateral surface roughness one ($R_{a\ lateral}$=2.553 µm).

Table 1.Roughness parameter (CoCrMo sample)

Measurement site	Roughness parameter	Value (µm)
Top face (x-y)	R_a	0.244
Top face	R_q	0.305
Lateral face (x-z)	R_a	2.553
Lateral face	R_q	2.924

The upper surface of the workpiece (laser processed top face) shows traces of powder or small dents (≈ 20-30 µm), Fig. 5.

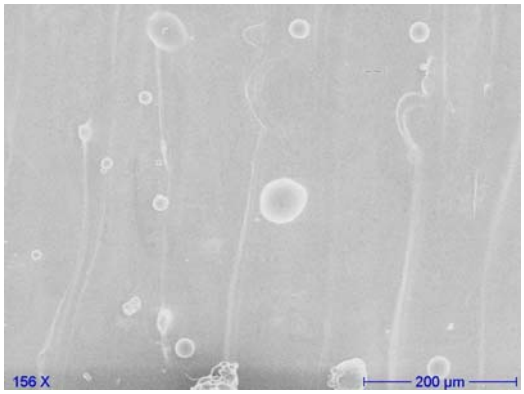

Fig.5. SEM micrograph of CoCrMo part (top surface)

As Fig. 6 illustrates, the maximum size of irregularities determining roughness are about. 30 µm, this size is comparable with the thickness of the sintered powder layer.

The continuous reduction in the size of the piece along a direction (from left to right in Fig. 6) suggests a slight dependence between deposited layer thickness and the general scanning direction performed by laser beam ("stair-step effect").

The distance between two successive maximum along x axis (roughness width) is significant (0.2 mm) in comparison with the amplitude irregularities and can be associated with laser sintered zone width in a single pass, which is approximated as 100-200µm.

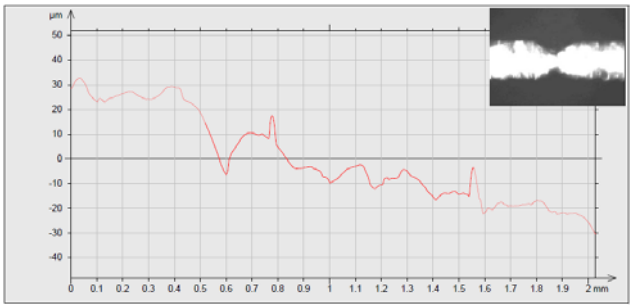

Fig. 6. CoCrMo Surface roughness profile of top face

The estimation is performed by analyzing the distances between the beam traces after scanning the workpiece surface, as seen in Fig. 5. Also, a detail is shown in Fig. 7.

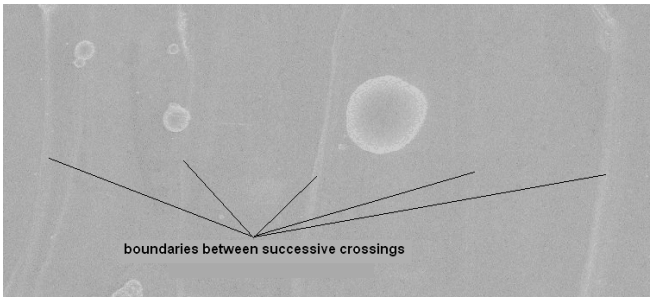

Fig. 7. SEM micrograph of CoCrMo part (Fig.5 detail) showing the fusion "traces" after laser beam scanning

Unlike the appearance of top surface profiles analyzed in the longitudinal direction of the workpiece (perpendicular to the beam scanning), the lateral profile is characterized by a smaller distance between two successive maximum (roughness width) as shown in Fig.8.

Such irregularities of surface are comparable in size with the powder particle sizes and can be associated with these particles sintered "partially melted" by the laser beam, which have been integrated more or less in lateral area.

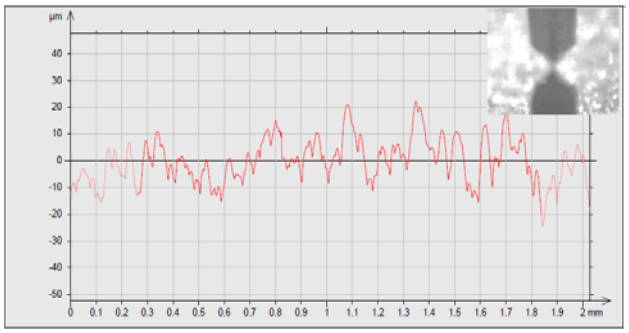

Fig. 8. CoCrMo surface roughness profile of lateral face.

The lateral surface is more irregular than the top surface.

Basically lateral boundaries profile consists of the powder particles profiles which were at the origin of the manufacturing. The rougher appearance is clearly revealed in the images of the lateral faces of the workpiece (Fig.9, Fig.10).

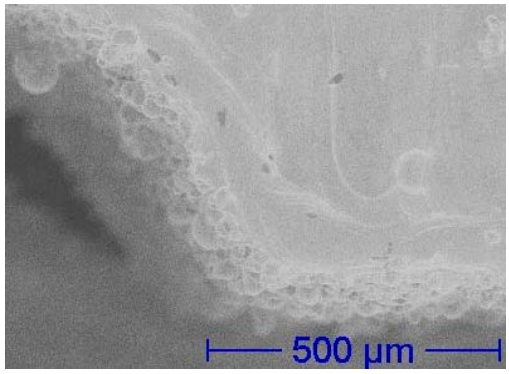

Fig. 9. SEM micrograph of a CoCrMo sample (the edge region).

The detail in Fig. 9 highlights the lateral region in which sintered powder particles can be noticed. Particles show in the highest proportion the 20-30 µm size, although can be highlighted some larger.

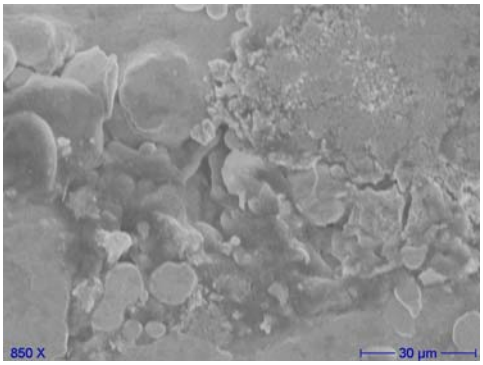

Fig.10. SEM micrograph of CoCrMo part (lateral surface).

3.2. Structural analysis of Ti6Al4V part

In comparison with the CoCrMo sample analysed above, the top surface of Ti6Al4V parts is rougher, with a higher number of defects (Fig. 11).

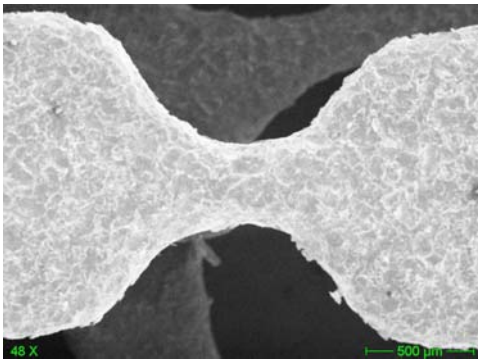

Fig.11. SEM micrograph of Ti6Al4V part (top face)

The surface texture, commonly known as "orange-peel" is main issue which affect part quality.

Unlike the CoCrMo sample, lateral and top surfaces topography of Ti6Al4V are similar (Fig. 12 a,b), and the roughness of these surfaces are significantly close ($R_{a\ top}$ =1.073 µm; $R_{a\ lateral}$ =0.751 µm), as can see in Table 2.

Table 2. Roughness parameter (Ti6Al4V sample)

Measurement site	Roughness parameter	Value (µm)
Top face (x-y)	R_a	1.073
Top face	R_q	1.301
Lateral face (x-z)	R_a	0.751
Lateral face	R_q	0.83

The lateral surface shown in Fig.12.b with a roughness $R_{alateral}$= 0.751 µm, seems better finished than lateral face of the CoCrMo sample ($R_{a\ lateral}$ =2.553 µm), but the top face (scanned by the laser beam) has a lower quality than the CoCrMo samples.

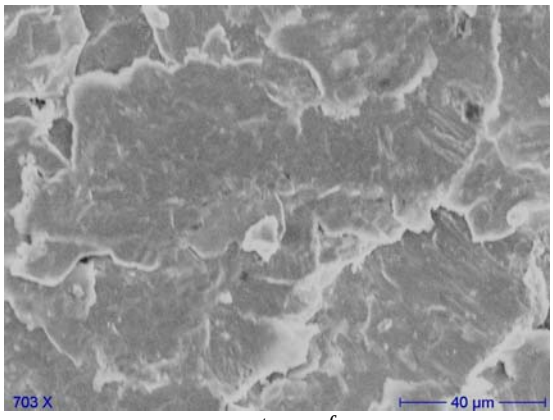

a. top surface

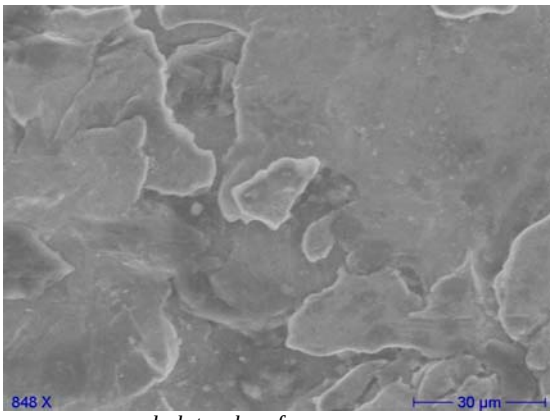

b. lateral surface

Fig.12. SEM micrograph of Ti6Al4v part

The part made in Ti6Al4V revealed an uniform morphology with irregularities which does not exceed 20 µm as can be observed in Fig. 13 and Fig. 14. It can be shown also a slight stair-step effect on the surface scanned by laser beam (Fig. 13).

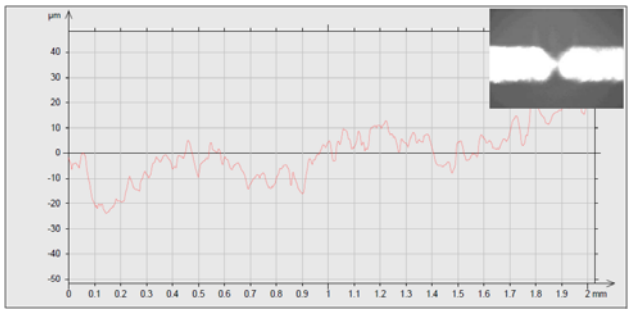

Fig.13. Ti6Al4V Surface roughness profile (top face)

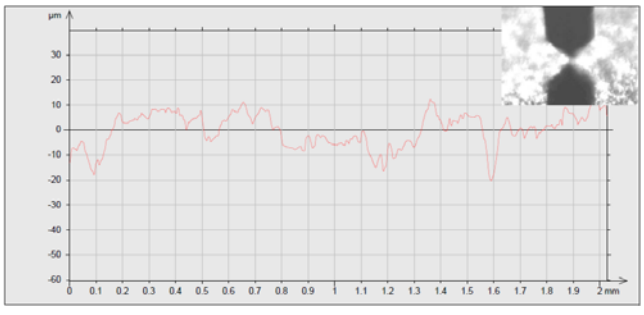

Fig.14. Ti6Al4V Surface roughness profile (lateral face)

4. Conclusions

Even if the dimensional accuracy and the surface quality of the parts manufactured by selective laser sintering is lower than the ones conventionally machined,

this technology is fast and flexible for 3D prototypes fabrication.

CoCrMo sample shows a large anisotropy (one order of magnitude) between the roughness of top surface and those of lateral surface ($R_{a\ top}$=0.244 μm; $R_{a\ lateral}$=2.553 μm). This difference is lower in case of Ti6Al4Vsample. The surface topography of parts made from this material seems to be more uniform.

The roughness of top surface ($R_{a\ top}$=1.073 μm) is closer to the roughness of lateral surface one ($R_{a\ lateral}$=0.751 μm).

For both parts, the upper surface (scanned by the laser beam) shows "a stair-step effect", a continuous reduction in the size of piece along a general scanning direction.

The differences in the top surface quality of CoCrMo and Ti alloy parts lead to the hypothesis that melting behaviour is significantly different or technological scanning procedure of the part surface by the laser beam is different.

Future works will be focused selective laser sintering of parts with a porosity gradient (variable from the bulk center to the external area which will be in contact with bone or a transient phase) or porous components with porosity and mechanical properties close to the bone properties.

Acknowledgement

The National Project, Young Research Teams, PN-II-RU-TE-2011-3-0299, no. 85/05.10.2011, "Advanced Devices for Micro and Nanoscale Manipulation and Characterization (ADMAN)".

The INCDMTM Institute for the selective laser sintering tests.

The FEMTO-ST Institute for the material characterisation facilities.

References

[1] X. Liu, P. K. Chu, C. Ding, Mat. Sci. Eng. R **70**, 275, (2010).
[2] A. A. Poinescu, R. M. Ion, R. I. Van Staden, J. F. Van Staden, M. Ghiurea, J. Optoelectron. Adv. Mater., **13**(3-4), 416, (2011).
[3] N. Angelescu, D. N. Ungureanu, A. Catangiu, Rev. Chim. Bucharest, **62**(7), 702 (2011).
[4] R. Roest, B. A. Latella, G. Heness, B. Ben-Nissan, Surf. Coat. Tech. **205**, 3520, (2011).
[5] L. N. Wang, J.L. Luo, Mater. Charact. **62**, 1076, (2011).
[6] L. Duta, F. N Oktarb, G. E. Stan, G. Popescu-Pelin, N. Serban, C. Luculescu, I. N. Mihailescu, Appl. Surf. Sci., **265**, 41, (2013).
[7] W. Suchanek, M. Yoshimura, J. Mater. Res. **13**, 94, (1998).
[8] X. Xinhong, Z. Haiou, W. Guilan, J. Mater. Process. Tech. **209**, 124 (2009).
[9] P. Amend, C. Pscherer, T. Rechtenwald, T. Frick, M. Schmidt, Phys. Proc. **5**, 561, (2010)
[10] I. G. Gheorghe, L. L Badita, J. Optoelectron. Adv. Mater., **13**(10), 1208 (2011).
[11] S. Bauer, P. Schmuki, K. Von der Mark, J. Park Prog. Mater. Sci., dx.doi.org/10.1016/j.pmatsci.2012.09.001, (2012).
[12] P. Rajesh, C. V. Muraleedharam, M. Komath, H. Varma, J. Mater. Sci. Mater. Med., **22**(7), 1671, (2011).

* Corresponding author: dumiver@yahoo.com